RSC Advances

ROYAL SOCIETY OF CHEMISTRY

www.rsc.org/advances

Journal Name

ARTICLE

Photoinduced curcumin derivative-coatings with antibacterial properties

Received 00th January 20xx,
Accepted 00th January 20xx

DOI: 10.1039/x0xx00000x

www.rsc.org/

M. Condat,[a] P.-E. Mazeran,[b] J.-P. Malval,[c] J. Lalevée,[c] F. Morlet-Savary, [c] E. Renard, [a] V. Langlois, [a] S. Abbad Andalloussi,[d] D.-L. Versace [*a]

The development of new antibacterial coating (against *Escherichia coli* and *Staphylococcus aureus*) with the use of a natural dye (curcumin) and epoxidized soybean oil, according to a photochemistry process has been investigated. Curcumin has been used both as a photosensitizer and an antibacterial agent under visible light illumination. The photoinduced coatings show good adherence properties on inox substrate and a high thermal stability by 375°C. Under visible light activation, singlet oxygen ($^1O_2$) could be generated from the curcumin derivative-coatings, thus inhibiting by 99% and 95% the growth of *Staphylococcus aureus* and *Escherichia coli,* respectively, even after 48h of incubation.

1. Introduction

Infections by pathogenic microorganisms are of great concern in many fields, particularly in medical devices, hospital surfaces/furniture, and surgery equipments. Approximately 64% of hospital-acquired infections worldwide are due to the attachment of bacteria to medical implants, and they are associated with an annual mortality of 100,000 persons in US as well as an increase in health-care costs[1, 2].

Persistence of clinically relevant bacteria on inanimate surfaces can remain up to several days and even months[3]. It is of great importance to interrupt this transmission pathway by a self-disinfecting effect of surfaces. To solve the problem of increasing resistance of bacteria much attention has been focused on developing new antimicrobial systems in biomedical industry. Therefore, new chemical strategies have been developed to prevent the bacterial colonization of materials surface. Four approaches could be cited: The first approach focused on reducing the capacity of bacteria to attach onto a surface[4-8]. The second approach is based on lethal contact which induces the biochemical death of bacteria[9-11]. The third approach has referred to the biocide leaching[12-16]. A final alternative method for disinfecting surfaces consists in using a coating that produces reactive oxygen species upon light activation, also called the method of photodynamic inactivation (PDI). In this method, a photosensitizer (PS) is excited by light, for further generating reactive oxygen species [17] (e.g. singlet oxygen, $^1O_2$), that can cause cell death[18-21]. In this context, PSs do not have to penetrate the bacterium or even come into a contact with the cell in order to be effective.

Antibacterial surfaces which work with the PDI principle are of great interest due to their preventive character for infections[22-24]. Such surfaces could help to reduce the transmission of multi-resistant microorganisms, which is of great importance in hospital hygiene[25]. It has been demonstrated that PSs destroy bacteria, viruses, fungi, yeasts and parasites upon illumination[26-28]. Gram positive bacteria seem to be however more susceptible to PDI than Gram negative bacteria[29, 30]. As such surfaces do not necessarily lead to PS consumption, self-disinfecting coatings could offer a constant prevention of microorganism adhesion and proliferation on any surface[31]. Many investigations have already been performed with porphyrins and phthalocyanine derivatives[32, 33], hydroxyethyl Michler's ketone[34], toluidine blue[35], eosin Y[36, 37], methylene blue[35, 38] or rose bengal[39].

[a] *Institut de Chimie et des Matériaux Paris-Est, Equipe Systèmes Polymères Complexes, UMR 7182, CNRS-Université Paris-Est Créteil Val de Marne 2-8 rue Henri Dunant – 94320 Thiais, France. Fax: +33 1 49 78 12 01; Tel: +33 1 49 78 12 28; E-mail: versace@icmpe.cnrs.fr.*
[b] *Laboratoire Roberval, UMR CRNS-UTC 7337, Centre de Recherche de Royallieu, Université de Technologie de Compiègne, 60205 Compiègne Cedex, France.*
[c] *Institut de Science des Matériaux de Mulhouse, IS2M-LRC 7228, 15 rue Starcky - 68057 Mulhouse, France.*
[d] *Unité Bioemco Equipe IBIOS, UMR 7618 CNRS - Université Paris-Est Créteil Val-de-Marne, 61, Avenue Général de Gaulle, 94010 Créteil cedex.*

Electronic Supplementary Information (ESI) available: Evolution of the absorbance of 1,3-diphenylisobenzofuran (DBF) and curcumin alone at 480 nm in acetonitrile under visible light illumination and emission spectrum of the 4 lamps used during the different incubation times. See DOI: 10.1039/x0xx00000x

To the best of our knowledge, no report has hitherto been published on the synthesis of antibacterial coatings under visible light activation using a natural dye, curcumin, which is used both as a photosensitizer and an antibacterial agent according to an environmentally substainable "photo chemistry" method.

Curcumin, the yellow-orange dye derived from the rhizomes of *Curcuma longa*, primary bioactive component of turmeric, has recently received attention from chemists due its wide range of potential applications ranging from pharmacology[40-43] (e.g. antioxidant, anti-inflammatory, anti-viral, anti-bacterial, anti-fungal, and antitumor activities) to its photobiological and photosensitizing actions[44-46]. More interestingly, it has also been reported that curcumin can act as a photoinitiator for free radical[47] and cationic[48, 49] photopolymerizations under air. However, the combination of the anti-bacterial and photosensitizing properties of curcumin has not been used yet for the synthesis of natural antibacterial coatings with highly thermal and mechanical strength.

In this paper, we present a new and simple route to efficiently synthesize an antibacterial coating derived from epoxidized soybean oil which is deposited on stainless steel plate and efficient enough to inhibit the bacteria growth, according to an environmentally-friendly method. The first part of this study demonstrates the photochemical properties of the photoinitiating system (curcumin and iodonium salt) through steady state, phosphorescence and fluorescence experiments. In a second part, a particular effort was made to characterize the synthesized coatings. For this purpose, the thermal and mechanical properties of the coatings were characterized by Thermo Gravimetric Analysis (TGA), nanoindentation and scratch tests. In addition, the generation of fluorescence through the curcumin derived coatings under visible light irradiation was investigated by fluorescence spectrophotometry. To validate the study, the antibacterial property of the synthesized coatings against *Escherichia coli* (*E. coli*) and *Staphylococcus aureus* (*S. aureus*) was evaluated.

2. Results and discussion

2.1 Photochemical properties. The absorption spectrum of curcumin in acetonitrile exhibits an absorption maximum at 420 nm (ϵ_{max}= 40000 M^{-1} cm^{-1}) which can be assigned to the π-π* transitions. In order to demonstrate the photosensitizer effect of curcumin onto iodonium salt (Iod), steady state photolysis experiments have been performed. Figure 1A describes the evolution of UV-visible absorbance of curcumin under different times of irradiation in the visible range. After 120s of irradiation, a decrease of only 10% of the total absorbance of curcumin was observed at 420 nm.

However when curcumin is irradiated in the presence of Iod (Figure 1B), the maximum absorbance peak for curcumin at 420 nm strongly decreases. Dramatic photobleaching was observed after only 30s of irradiation, thus demonstrating that the photoinitiating system curcumin/Iod is highly reactive.

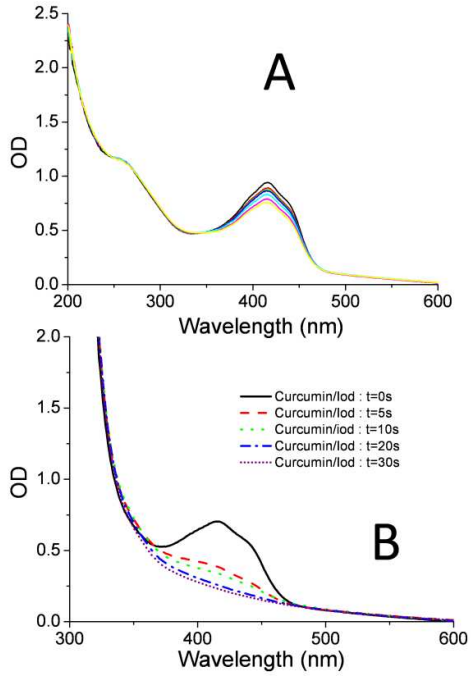

Fig. 1. Steady state photolysis of A) curcumin during 120s of irradiation [Curcumin] = 2.8 x 10^{-5} mol/L in acetonitrile and B) curcumin/Iod during 30s of irradiation. [Curcumin] = 2 x 10^{-5} mol/L; [Iod] = 2.6 x 10^{-2} mol/L. Lamp Xenon. I = 30 mW.cm^{-2}.

The ability to generate protons using curcumin as visible photosensitizer of Iod is illustrated in Figure 2. In this experiment, both compounds are mixed together in acetonitrile (ACN) in presence of rhodamine B (RhB) as acid indicator[50]. As shown in Figure 2A, the irradiation of the solution at 420 nm leads to a gradual decrease of the longest wavelength absorption band of curcumin in concomitance with the growth of the lowest energy band of the acid form of RhB at 550 nm. It should be emphasized that the irradiation of Iod without curcumin and in the same conditions does not generate any protons. Reciprocally, the irradiation of curcumin without Iod does not induce any acid generation as depicted in Figure 2B (see the inset). It should be noted that the presence of Iod (charged molecule) increases the ionic strength force of the solution, thereby leading preferentially to the formation of the rhodamine B in its acid form at t = 0s (see Figure 2A). On the contrary, without Iod in solution, RhB remains in its basic form at t = 0s.

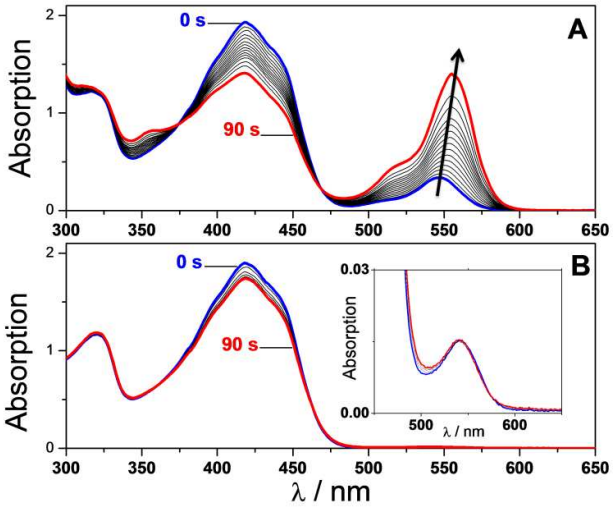

Fig. 2. Evolution of the absorption spectrum of curcumin ($3.6x10^{-5}$ M in non degassed ACN) (λ_{ex} : 420 nm). A) In the presence of Iod ($1.5x10^{-3}$ M) and B) Without Iod. Both solutions contain Rhodamine B base ([RhB] = 1×10^{-5} M) which is used as acid indicator. Inset: Evolution of the absorption spectrum of RhB band at 550 nm during irradiation of (curcumin/RhB) solution. I = 30 $mW.cm^{-2}$.

Finally, the presence of oxygen in the solution clearly has a detrimental effect in the efficiency for acid photogeneration. Figure 3 shows the time evolution of the absorbance at λ_{max} of the acid form of RhB for nitrogen saturated and non degassed solutions. One clearly observes a strong enhancement by a factor 7 for the initial of H^+ photogenerated for nitrogen saturated solution. Such an oxygen inhibition effect indirectly suggests that the photosensitization of Iod by excited curcumin mainly proceed through its triplet excited state. The quantum yield for the H^+ photogeneration (Φ_{H+}) has been evaluated at 0.01 according to the method reported by Scaiano et al[51].

The free energy change ΔG_T for the ^{3}Curcumin/Iod electron transfer reaction is highly reactive and make the process favourable according to the Rehm-Weller equation[52] (eq 3): -1.20 V (E_{ox} of curcumin = 0.78 eV as measured by cyclic voltammetry in this work; E_{Red} of Iod = -0.2V[53], triplet state energy E_T of curcumin = 1.95 eV as extracted from the phosphorescence spectrum (Figure 4).

Figure 4 displays the time-gated phosphorescence spectrum of curcumin in glassy matrix of ethanol (77 K). The maximum luminescence is located at 636 nm leading to a lowest triplet state energy of ca. 1.95 eV. The phosphorescence lifetime of about 14 µs (see inset Figure 4) is also a clear indication of an emissive triplet state having strong n,π* character.

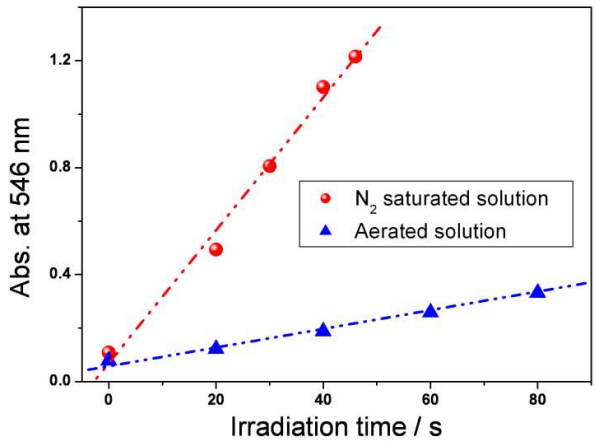

Fig. 3. Plots of the absorbance at λ_{max} of RhB (acid form) as function of the irradiation time (λ_{ex} : 430 nm) for degassed and non degassed solutions of acetonitrile ([Curcumin] = $3.6x10^{-5}$ M, [Iod] = $1.5x10^{-3}$ M, [RhB] = $1x10^{-5}$ M). I = 30 $mW.cm^{-2}$.

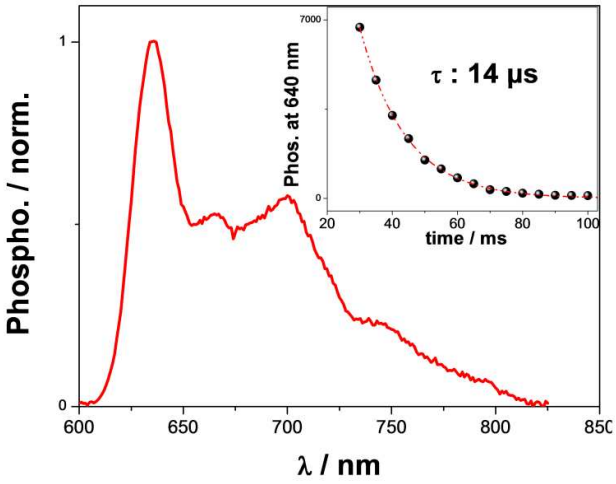

Fig. 4. Normalized phosphorescence spectrum of curcumin in glassy matrix of ethanol (λ_{ex}: 435 nm, recording delay after pulse excitation: 30 µs). Inset: Decay profile of the phosphorescence signal monitored at 640 nm.

Even if the triplet energy transfer between curcumin and Iod seems to be the main process, the singlet energy electron transfer could be a second way according to the fluorescence experiments. The fluorescence emission of curcumin in acetonitrile is described in Figure 5. The blue curve corresponds to the absorbance spectrum of curcumin in its fundamental state with a maximum absorption at 420 nm. The red curve corresponds to the emission spectrum of curcumin with a maximum at 520 nm. The crossing of the two curves corresponds to a λ_{fluo} at 460 nm.

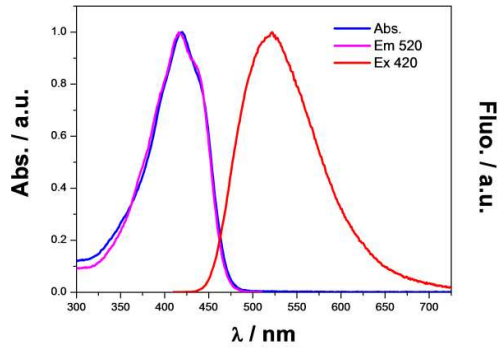

Fig. 5. Absorbance and emission spectra of curcumin in acetonitrile. The blue curve corresponds to the ground state absorption spectrum of curcumin. The red curve corresponds to the emission spectrum of curcumin. Excitation at 420 nm.

In the presence of Iod, the fluorescence of curcumin at 520 nm is quenched by electron transfer reaction (Figure 6). A quenching constant $k_q\tau_0$, between curcumin and Iod, was evaluated at 16.2 ± 0.2 M^{-1}. As the fluorescence lifetime of curcumin[45] τ_0 was evaluated at 376-695 ps in acetonitrile; therefore k_q is around 3 x 10^{10} M^{-1} s^{-1}. The large interaction rate constant k_q indicates that the process is almost diffusion-controlled.

The free energy change ΔG_S for the ^{1}Curcumin/Iod electron transfer reaction is favourable according to the Rehm-Weller equation[52] (eq 1): -1.72 V (E_{ox} of curcumin = 0.78 eV as measured by cyclic voltammetry in this work; E_{Red} of Iod = -0.2V[53], singlet state energy E_S of curcumin = 2.7 eV as extracted from the UV-vis absorption and fluorescence emission spectra).

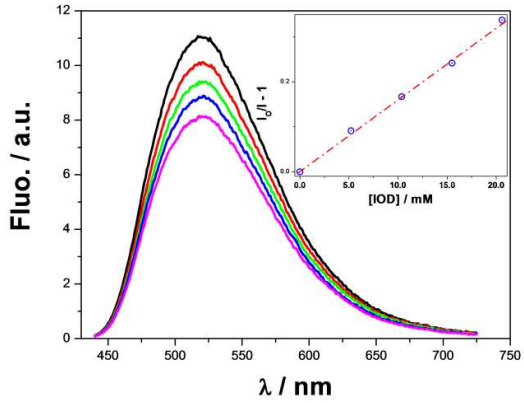

Fig. 6. Fluorescence quenching of curcumin by Iod in acetonitrile. Inset: evolution of the fluorescence intensity as a function of [Iod].

2.2 Synthesis of the coatings. For the first time, the photochemical reactivity of the photosensitive formulation containing epoxidized soybean oil /curcumin/Iod was evaluated with the use of RT-FTIR by following the decrease of the epoxy group through visible illumination at 810 cm^{-1} (Figure 7A). During irradiation, the intensity of the epoxy group strongly decreases and a new peak at 1080 cm^{-1}, corresponding to the formation of a polyether network, was observed, thus demonstrating the photopolymerization of the epoxidized soybean oil (Figure 7B). The final epoxy conversion at 600s is 80%. The coating is totally take-free: an optical image of the coating which is deposited on an inox substrate is displayed on Figure 8.

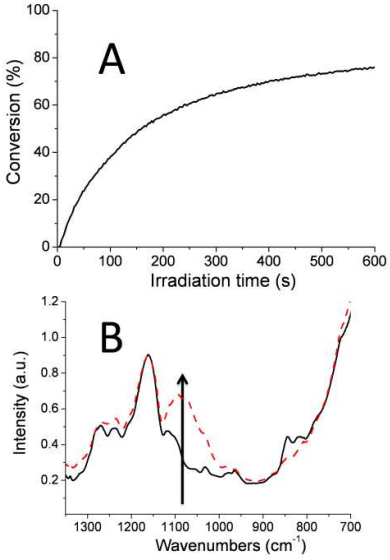

Fig. 7. A) Photopolymerization kinetic of epoxidized soybean oil under light activation and B) IR spectrum of coating before (solid line) and after 600s of irradiation (dot line). Xe lamp, intensity= 30 mW/cm^2, distance 6 cm, film thickness = 100 µm.

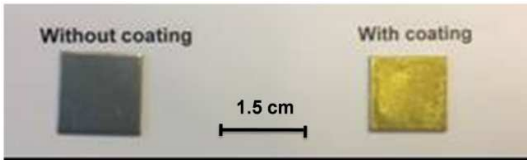

Fig. 8. Optical image of the inox plate (left) and the curcumin derivative-coating deposited on an inox plate.

2.3 Thermo Gravimetric Analysis (TGA). Thermal stability of the coatings was studied by Thermal Gravimetric Analysis (TGA), under oxygen atmosphere. The results are displayed in Figure 9. It can be observed that the coating reached 50% weight loss at 370°C.

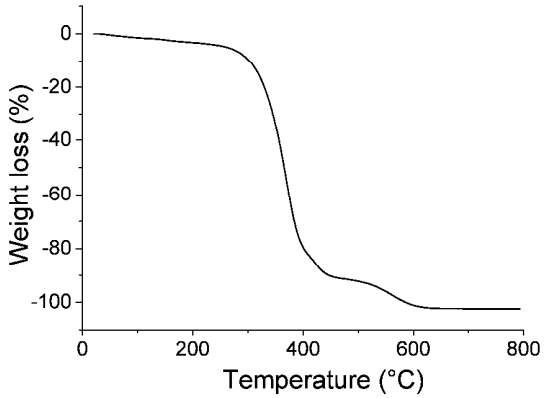

Fig. 9. TGA thermogram of the photoinduced curcumin coating under oxygen atmosphere.

2.4 Nanoindentation and scratch tests. The loading and unloading curves during the nanoindentation tests are closed to be superimposed showing that the coatings have at room temperature a quasi-viscoelastic behavior indicating that the polymer is in a rubber-like state at room temperature. The elastic modulus as measured by the Continuous Stiffness Measurement (CSM) method was found to be around 105±12 MPa and 130±12 MPa for the inox substrate and glass substrate respectively (Means ± Standard deviation). Concerning the scratch tests, the comparison of the height profiles before and after scratch tests reveals the recovery of the material confirming the rubber-like behavior (Figure 10). A bulge on the height profile during and after scratch evidences the apparition of the brittle fracture of the film. The critical load is 70±27 mN and 58±32 mN for the steel and glass substrate respectively (Means ± Standard deviation). On glass, brittle fractures of the film do not lead to delamination showing a good adherence to the substrate (Figure 11A), on the opposite, delamination occurs during scratch test showing a weaker adherence of the film on the substrate in comparison with glass substrate (Figure 11B.

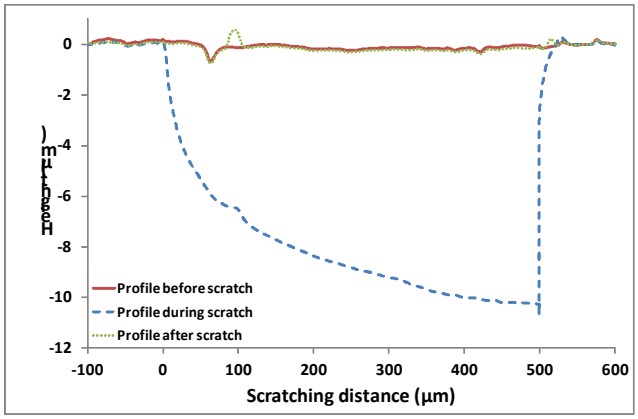

Fig. 10. Height profile before, during and after scratch test on the curcumin derivated coating deposited on glass substrate. The bulge on the profile after scratch evidences the beginning of the fracture.

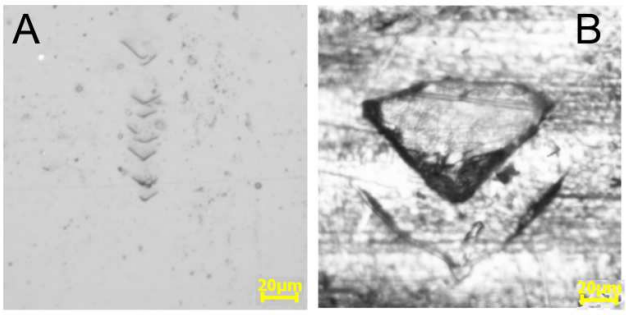

Fig. 11. Scratch resistance on A) the glass substrate and B) on the modified stainless steel plate. Scratch tests have been performed face forward on a length of 500 µm with an increasing load (0 to 100 mN from bottom to top).

2.5 Fluorescence of the coating. After irradiation of the curcumin derived formulation (600s), free curcumin dyes left embedded inside the coating as demonstrated by UV-vis spectrometry (Figure 12) and epifluorescence (Figure 13). The fluorescence of the film which stems from the remaining curcumin suggests that excitation of this chromophore can be used to efficiently generate singlet oxygen as it will be highlighted in the following section.

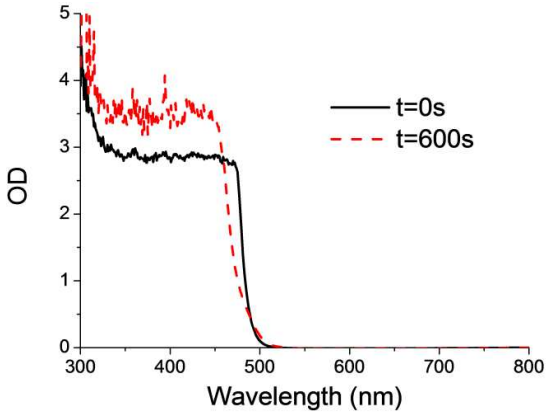

Fig. 12. Evolution of the UV-vis spectra of the curcumin derivative-coating after 600s of irradiation. Xe lamp, intensity = 30 mW/cm^2. Formulation was sandwiched under 2 glass substrates.

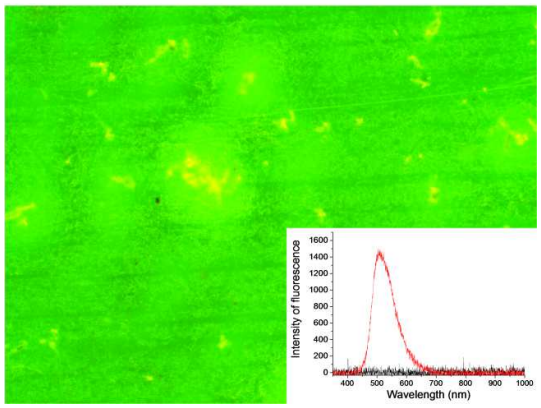

Fig. 13. Epifluorescence of curcumin located into the polymer coating after 600s of irradiation (lamp Hg-Xe, intensity = 30 mW/cm^2). Inset= fluorescence intensity of the curcumin located into the coating after polymerization.

2.6 Antibacterial property. Prior to investigate the antibacterial effect of the curcumin derivative-coatings, the ability of curcumin to inhibit the bacterial proliferation in solution was investigated against Gram-Negative (*E. coli*) and Gram-Positive (*S. aureus*) bacteria after 2h, 6h, 24h and 48h, with and without irradiation in the visible range. Initially, 3x10^6 CFU/mL of each bacteria was introduced in solution or put into contact with coatings at t = 0h.

First, a reference study referring to the light irradiation against the two bacteria strains was performed (Figure 14). The results show that the irradiation does not have any influence on the growth of *E. coli* and *S. aureus*. A second reference study was done in the presence of DMSO, because curcumin is not soluble in water. According to the first results, DMSO does not affect the bacterial activity as the decrease of CFU is not significant whatever the stains used.

The antibacterial effect of curcumin was then done in DMSO, under light activation. The irradiation of curcumin leads to an antibacterial effect on both strains: indeed, the irradiated curcumin solutions allow the total death of *S. aureus* after 6h of incubation and 99% inhibition of *E. coli* growth after 2h of incubation. The antibacterial effect against the both bacteria strains remains efficient even after 48h. The variation in curcumin killing efficacy at different exposure durations was found to be statistically significant (p value < 0.05 on comparing percentage survival). Without irradiation, more than half of bacteria are always alive after 48h of incubation for both bacteria.

These results confirm the inactivation or lysis of *S. aureus* and *E. coli* according to two processes. *E. coli*, a gram negative bacteria, have one or a few layers of peptidoglycan and an external membrane with lipoproteic character[35]; thus allowing the hydrophobic components (like curcumin) to penetrate the membrane and leading to its alteration by disruption. On the contrary, gram positive bacteria (*S. aureus*), protect their cytoplasmic membrane with a thick multilayer peptidoglycan wall that blocks the introduction of hydrophobic components because of the presence of amino acids and sugars within the cell membrane[35]. Therefore, only hydrophilic components penetrate the wall. So, a second interesting explanation could be pointed out from our antibacterial results. Some reports concerning the inactivation of bacteria demonstrate that photosensitizers do not have to penetrate the cell membrane or even to come into contact to be effective. Indeed, if sufficient quantities of singlet oxygen can be generated near the outer membrane of the bacteria, it will lead to its damage[54]. In our investigation, Electron Paramagnetic Resonance (EPR) spectroscopy was used to monitor the $^1O_2$ generation ability of curcumin upon photo-illumination in the visible range. Amount of 2,2,6,6-tetramethylpiperidine (TEMP), a diamagnetic molecule, was used to capture singlet oxygen by yielding a paramagnetic product, the nitroxide radical TEMPO[17, 55, 56]. As shown in Figure 15, the EPR spectral signal of three lines of equal intensity, which is attributed to the TEMPO nitroxide radical, was observed when an oxygen-saturated solution of curcumin was irradiated in the presence of TEMP at room temperature. Upon photoirradiation of curcumin, the intensity of the EPR signal increases gradually, indicating the formation of $^1O_2$ molecules.

The quantum yield for singlet oxygen generation (Φ_Δ) upon excitation of curcumin has been evaluated in ethanol based on a photoxidation method using 1,3-diphenylisobenzofuran (DBF) as $^1O_2$-sensitive indicator[57]. Rose Bengal[58] (RB) was employed as a standard photosensitizer (Φ_Δ^* = 0.68 in ethanol) and isoabsorbant solutions of curcumin and RB solutions were irradiated at 480 nm. Both ethanolic solutions contained DBF at 5 x 10^{-4} M. The absorbance of DBF at 327 nm was recorded at different irradiation times as displayed in Figure 16. At 480 nm, DBF weakly absorbs and the absorbance of DBF alone or curcumin alone remains constant under visible light activation as demonstrated in Figure S1. The value of $\Phi_\Delta/\Phi_\Delta^*$ is obtained from the ratio of the corresponding slopes at initial time of irradiation. A value of 0.05 is therefore measured for the $^1O_2$ photogeneration quantum yield by curcumin.

According to these results, it is likely that the curcumin which have been introduced into the synthesized coatings could generate singlet oxygen to inhibit the bacteria growth on stainless steel substrates. This is well supported by the fact that no curcumin is released from the polymeric coatings after the different incubation times, when coatings are introduced in aqueous bacteria solution. This phenomenon could be explained by the high final polymerization conversion of the epoxidized soybean oil after visible light irradiation.

The ability of the curcumin derivative-coatings (deposited on stainless steel substrates) to inhibit the bacteria adhesion was investigated in comparison with the unmodified stainless steel substrates, and the curcumin-derivative coatings with and without light activation (Figure 17). A quantitative method for quantifying the total biofilm population has been used as reported by many antibacterial investigations[11, 59, 60]. According to Figure 17, the antibacterial effect is more efficient against *S. aureus* than for *E. Coli* under light activation. After 2h, the number of CFU *S. aureus* decreases, whereas it strongly increases on the unmodified stainless steel plate. After 24h and 48h of incubation, 99% inhibition of *S. aureus* growth is observed. For *E. coli*, the antibacterial activity of the coating begins after 6h of incubation (Figure 17) but remains less efficient than for *S. aureus*. Indeed, only 80% and 95%

inhibition of *E. coli* growth are demonstrated after 24h and 48h respectively. Another interesting result is the increase of the bacteria population on the curcumin-derivative coatings without visible light illumination and whatever the bacteria strains used. This later result demonstrates that light is essential for leading to an antibacterial effect.

This experiment finally demonstrates the efficiency of the coating to strongly diminish the adherence/proliferation of two bacteria strains on the stainless steel supports by generating reactive oxygen species ($^1O_2$ molecule). It is worth noticing that the live/dead assay for evaluating the death of bacteria in this case is not really suitable because of the intense fluorescence of the polymeric coatings due to the presence of curcumin.

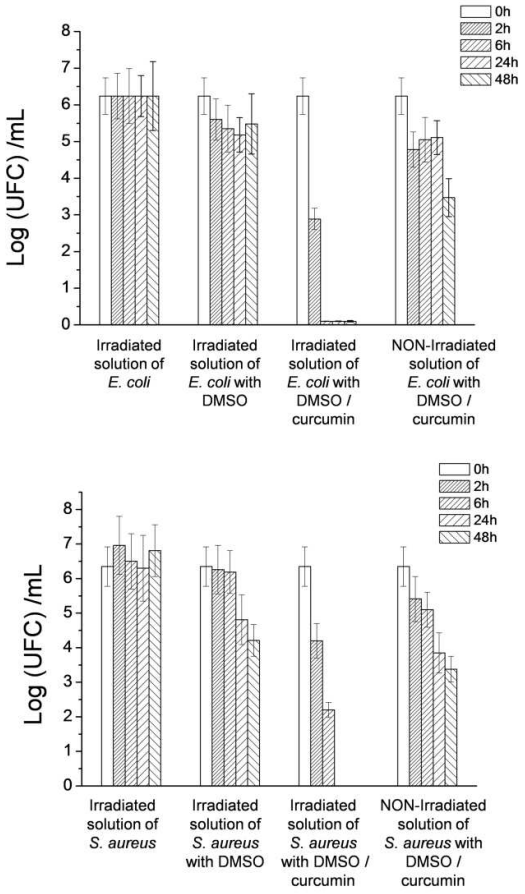

Fig. 14. Influence of the incubation time (0, 2, 6, 24 and 48 h) and the irradiation on the growth of a) *E. coli* and b) *S. aureus*. [Curcumin] = 160 µM.

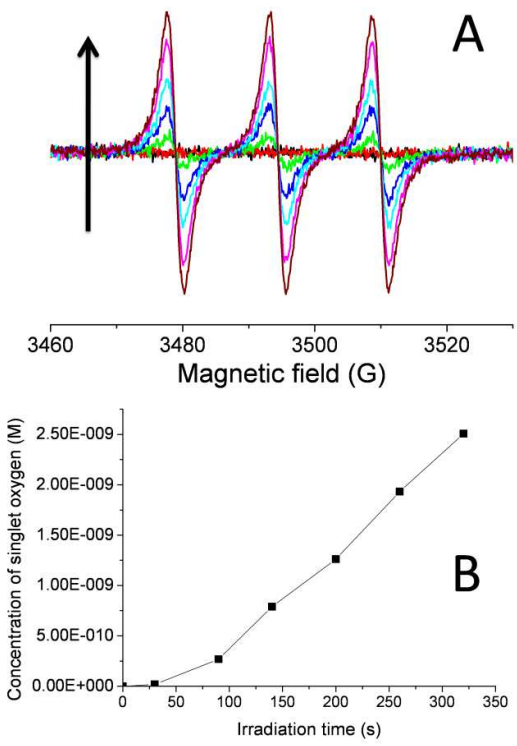

Fig. 15. A) EPR spectra obtained under light irradiation of curcumin in *tert*-butylbenzene in aerated conditions after 320s. The increase of the EPR spectrum is ascribed to the 2,2,6,6-tetramethyl-1-piperidinyloxy radical (TEMPO). B) Evolution of the generated singlet oxygen in solution during light activation.

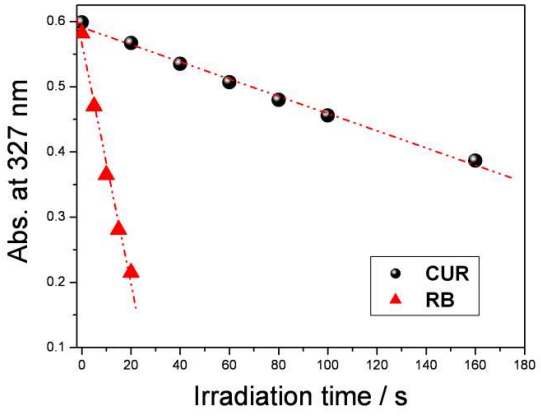

Fig. 16. Evolution of the absorbance of 1,3-diphenylisobenzofuran (DBF) at 327 nm as function of the irradiation time (λ_{ex} = 480 nm). [DBF] = 5 x 10^{-4} M in ethanol. CUR = curcumin and RB = rose benghal.

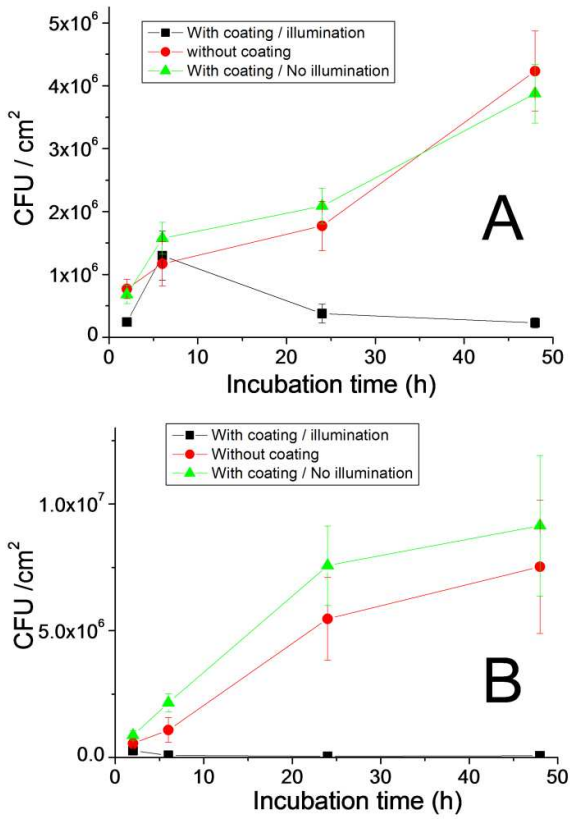

Fig. 17. Comparison of the antibacterial property of the stainless steel substrate (circle), the stainless steel plate with the curcumin-derivative coating under visible light illumination (square) and the stainless steel plate with the curcumin-derivative coating without visible light illumination (triangle) against A) *E. coli* and B) *S. aureus*.

3. Experimental

Materials. Curcumin (≥65%), epoxidized soybean oil (ESBO), 2,2,6,6-Tetramethyl-1-piperidinyloxy (98%, TEMPO), 2,2,6,6-Tetramethylpiperidine (≥ 99%, TEMP), Rose Benghal (RB, 95%), Rhodamine B (RhB, ≥ 95%) and 1,3-diphenylisobenzofuran (DBF, 97%) were purchased from Sigma Aldrich. Iodonium 4-(2-methylpropyl)phenyl-hexafluorophosphate (Iod, Irgacure ®250) was purchased from Badische Anilin und Soda Fabrik (BASF). Acetonitrile (ACN), ethanol (EtOH) and toluene were supplied by Sigma Aldrich (HPLC grade). The main compounds used in this study are displayed in Table 1. Stainless steel substrates were cut on large stainless steel plate to obtain the plate size of 1.5 x 1.5 cm.

Table 1. Structure of the monomer and photoinitiating systems used in this study.

Compound	Function	Structure
Epoxidized soybean oil	Monomer	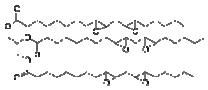
Curcumin	Photosensitizer and antibacterial agent	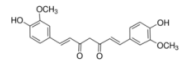
Iodonium 4-(2-methylpropyl)phenyl-hexafluorophosphate (Iod)	Cationic photoinitiator	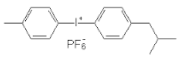
1,3-diphenylisobenzofuran (DBF)	Determination of $^1O_2$	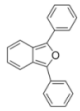
2,2,6,6-Tetramethylpiperidine (TEMP)	Singlet oxygen scavenger	
2,2,6,6-Tetramethyl-1-piperidinyloxy (TEMPO)	Determination of $^1O_2$	
Rhodamine B (RhB)	Acid indicator	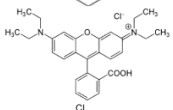
Rose Benghal	Standard photosensitizer for the determination of $^1O_2$ photogeneration quantum yield	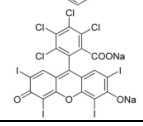

Steady state photolysis experiments. Curcumin, in the presence of additive (i.e. Iod) in acetonitrile, was irradiated with the Xenon lamp, and the UV-vis spectra were recorded on a Varian spectrophotometer (cary50 bio) in the range 250 nm to 800 nm in acetonitrile.

Determination of the quantum yield acid generation. The method has been previously described by Scaiano et al[51]. More precisely, the quantum yields for acid generation were measured under irradiation at 420 nm using a 200 W Xenon Lamp (Hamamatsu, L8-03) equipped with a band pass. The irradiated curcumin/Iod solution in acetonitrile was previously N_2 degassed. The progress of the photoreaction was monitored via UV-vis absorption spectra.

The acid generation in acetonitrile was evaluated from a calibration curve of Rhodamine B (used as a sensor of photoacid generation) which was gradually protonated by addition of p-toluenesulfonic acid[61]. Then, photoacid quantum yields were calculated according to the equation 1:

$$\Phi_{H^+} = \frac{V_{sol}}{l_{cell} S_{irr}} \frac{\frac{N_A}{\varepsilon_{RhB}} \left| \frac{dA_{550\ nm}}{dt} \right|}{I_0 \left(1 - 10^{-A_{420\ nm}}\right)} \qquad \text{(Eq 1)}$$

where V_{sol}, l_{Cell} and S_{irr} correspond to the volume of the irradiated solution, the optical path and the irradiated surface respectively. N_A is the Avogadro number. $A_{550\ nm}$ and ε_{550nm} is attributed to the absorbance and the molar extinction coefficient of Rhodamine B. Finally, the incident light intensity at 420 nm (I_0) was measured by ferrioxalate actinometry[62].

Electron Paramagnetic Resonance (EPR) experiments. EPR experiments were carried out using the Bruker EMX plus X-Band

EPR Spectrometer. The radicals were generated at room temperature upon LED exposure (420 nm) under air.

Photopolymerization procedure. For the cationic photopolymerization, 6.6 mg of Iod (2.2 wt % with respect to the epoxy monomer) 18.0 mg of curcumin (6 wt % with respect to the epoxy monomer) was dissolved into epoxy monomer formulation (ESBO, 300 mg) containing 150 µL of acetonitrile. Kinetics of photopolymerization were followed by Real Time Fourier transform infrared spectroscopy (RT-FTIR) using a Thermo-Nicolet 6700 instrument. The liquid samples were applied to a BaF_2 chips by means of calibrated wire-wound applicator. The thickness of the UV-curable film was evaluated at 100 µm. The RT-FTIR analyses were carried out under air conditions. Samples were irradiated at room temperature, by means of a Lightningcure LC8-03 lamp from Hamamatsu, equipped with a xenon lamp (200 W) coupled with a flexible light guide. The end of the guide was placed at a distance of 6 cm. The maximum UV light intensity at the sample position was evaluated to be 30 mW/cm^2. The photopolymerization was monitored by the disappearance of the epoxy function of the ESBO monomer at 910 cm^{-1}. The decreases of epoxy function at 910 cm^{-1} and the increasing of polyether at 1080 cm^{-1} demonstrate the efficiency of the photopolymerization. Conversion rate was calculated with the equation 2:

$$\text{Epoxy conversion (\%)} = (A_0 - A_t) / A_0 \quad \text{(Eq 2)}$$

A_0 represents the area at t=0s, and A_t represents the area at any time t.

Coatings preparation. Prior to the deposition of formulation on stainless steel plate, the later has been intensively cleaned with ethanol and toluene. The photosensibilized formulation containing ESBO, Iod and curcumin (100 µL) were then deposited and spin-coated on the dried stainless steel substrates. Both sides of stainless steel plate were irradiated at a distance of 6 cm at room temperature by means of a Lightningcure LC8-03 lamp from Hamamatsu, equipped with a xenon lamp (200 W) coupled with a flexible light guide. The irradiation time was fixed at 600 s per side with an intensity of 30 mW/cm^2.

Thermo Gravimetric Analysis (TGA). 10 mg of the coating were introduced into aluminium pans and was analyzed using on a Setaram Setsys Evolution 16 thermobalance by heating the sample from 20 °C to 800 °C with a heating rate of 15 °C/min, under air.

Fluorescence. The absorption measurements were carried out with a Perkin-Elmer Lambda 2 spectrometer. Steady-state fluorescence spectra were collected from a FluoroMax-4 spectrofluorometer. Emission spectra were spectrally corrected. The interaction rate constants kq between curcumin and Iod were extracted from Stern Volmer treatment ($I_0/I = 1+k_q\tau_0$ [Iod]; where I_0 and I stand for the fluorescence intensity of curcumin without and with the presence of Iod, respectively; τ_0 stands for the lifetime of curcumin without Iod).

Phosphorescence. Phosphorescence measurements were performed in ethanol at 77 K. The samples are placed in a 5 mm diameter quartz tube inside a Dewar filled with liquid nitrogen. The phosphorescence lifetimes were measured using a FluoroMax-4 spectrofluorometer, which is also equipped with a Xe-pulsed lamp operating at up to 25 Hz. The phosphorescence decays are obtained according to a time-gated method. The emission is recorded using a control module that includes a gate-and-delay generator that allows the integration of the signal during a specific period after a flash (delay) and for a predetermined time window. The total signal is accumulated for a large number of exciting pulses.

Fluorescence microscopy. Inverted microscope IX73 from Olympus equipped with a 75W Xe Lamp housing. The excitation and emission light is filtered with a fluorescence mirror unit (U-FUN from Olympus) associating a band pass filter centered at 365 nm (BP360-370), dichroic mirror (DM410) and long pass filter (BA420IF).

Redox potentials. The oxidation potential (E_{ox} vs SCE) of the studied curcumin was measured in acetonitrile by cyclic voltammetry with tetrabutylammonium hexafluorophosphate (0.1 M) as supporting electrolyte (Voltalab 6 Radiometer). The working electrode was a platinium disk and the reference electrode was a saturated calomel electrode (SCE). The free energy change ΔG for an electron transfer between the studied compounds and Iod can be calculated for the classical Rehm-Weller equation (Eq 3, where E_{ox}, E_{red}, E_s (or E_T), C are the oxidation potential of the studied compounds, the reduction potential of Iod, the excited (or triplet) state energy of the studied compounds, and the electrostatic interaction energy for the initiatlly formed ion pair, generally considered as negligible in polar solvents[52]:

$$\Delta G = E_{ox} - E_{red} - E_S \text{ (or } E_T) + C \quad \text{(Eq 3)}$$

Nanoindentation and scratch tests. Nanoindentation and scratch tests were carried out on the coatings (deposited on glass and steel substrates) with a Nano Indenter (Agilent Technologies G200) using a Berkovich tip (Micro Star Technologies). Twenty Nanoindentation tests per sample were performed. Samples were loaded and unloaded at constant strain rate (0.05 s^{-1}) using the Continuous Stiffness Measurement (CSM) method until an indentation depth of 1 µm. The unloading stage was performed after a hold load plateau of 300s in order to exhibit the viscous behaviour. Twenty scratch tests were performed; face forward, with an increasing load from 0.1 to 100 mN for a scratching distance of 500µm. The distance between two scratches was fixed to 500µm.

Antibacterial property of the coatings. Initial adhesion assays were performed using two strains of bacteria, namely *E. coli* ATCC25922 and *S. aureus* ATCC6538 on the curcumin derivative-coatings. Prior to in vitro antibacterial tests, the bacterial strains were grown aerobically overnight in Luria–Bertani broth at 37 °C under stirring. Overnight cultures of *E. coli* and *S. aureus* grown in Luria–Bertani (LB) broth were diluted to an optical density (OD 600 nm) of 0.05 in sterile LB broth. At this point, the inox supports and inox substrates with coatings (1.5 cm x 1.5 cm) were immersed in the culture; the corresponding vials were placed on a slantwise rotating wheel to avoid the sedimentation of bacteria, incubated for different times (2h, 6h, 24h and 48h) and shaken at 150 rpm to allow initial adhesion to occur (INFORS AG-CH 4103, Bottmingen-Basel, Switzerland). During the incubation time, some samples are illuminated with 4 lamps (intensity = 170 $\mu mol/m^2/s$). The emission spectrum is given in Figure S2. Following adhesion, the samples were rinsed seven times with sterile saline solution (NaCl, 0.9% w/v) to remove any non-adherent cells.

Colonized native and treated samples were then transferred to 2 ml sterile saline (solution A) and vortexed vigorously for 30 s. The samples were then transferred to 2 ml sterile saline (solution B) and sonicated in a Branson 2200 sonicator for 3 min. Samples were transferred once more to 2 ml sterile saline (solution C) and vortexed vigorously for 30 s. Suspensions A, B and C were pooled, serially diluted and plated on PCA medium for viable counting. The cells removed during these three phases represent the loosely attached biofilm population. A 100 µL volume of the detached viable bacteria solution was introduced onto the surface of a Plat Count agar plate. The process was repeated through a succession of 24 pre-dried substrates. Finally, the total bacterial adhesion was determined by a counting of the CFUs, after overnight statically incubation of the agar plates at 37 ° C. Each experiment was done four times. Levels of adhesion were given as numbers of cells per square centimeter.

Antibacterial property of curcumin in solution. The reference solution (bacteria/DMSO) and the curcumin solution in DMSO (160 µM) containing bacteria were placed on a slantwise rotating wheel to avoid sedimentation of bacteria, incubated for 2h, 6h, 24h and 48h at room temperature under visible illumination or not. The volume of DMSO corresponds to 3% v/v of the total bacteria solution. The process is the same as described in the previous paragraph. The suspensions were pooled and serially diluted. A 100 µL volume of the viable bacteria solution was introduced onto the surface of a Plat Count agar plate.

Finally, the number of viable bacteria was determined by a counting of the CFUs, after overnight statically incubation of the agar plates at 37°C. Each experiment was done four times.

Statistical analysis. All values corresponding to the anti-adherence property of *E. coli* and *S. aureus* are expressed as mean ± standard deviation. Statistical analysis was performed using Student's *t*-test for the calculation of significance level of the data. Differences were considered statistically significant at $P < 0.05$. Ten samples per group were evaluated.

Conclusions

This investigation demonstrates for the first time, the ability of curcumin to be used both as a photosensitizer and an antibacterial agent (even incorporated in a coating) against *E. coli* and *S. aureus*. The resulting coatings derived from the epoxidized soybean oil which have been synthesized under visible light illumination, display a good adherence properties on stainless steel substrates and a high thermal stability by 375°C.

The synthesized coatings containing curcumin led under visible light activation to a reduction of the *S. aureus* and *E. coli* growth by 99% and 95% respectively, after 48h of incubation. This new coating could successfully be used to avoid bacteria proliferation and deposited on paramedical devices like disposable clamp or disposable scalpel which have only one-time use for few hours.

Acknowledgements

We would like to thank CNRS institute and University of Paris-Est Creteil for financial support and Léon Pereira for the cutting process of stainless steel substrates.

References

1. R. M. Klevens, J. R. Edwards, J. C. L. Richards, T. C. Horan, R. P. Gaynes, D. A. Pollock and D. M. Cardo, *Public Health Rep.* , 2007, 122, 160-166.
2. M. F. Sampredo and R. Patel, *Infect. Dis. Clin. N. Am.* , 2007, 21, 785-819.
3. B. Hota, *Clin. Infect. Dis.* , 2004, 39, 1182-1189.
4. I. P. Parkin and R. G. Palgrave, *J. Mater. Chem.*, 2005, 15, 1689-1695.
5. J. Genzer and K. Efimenko, *Biofouling*, 2006, 22, 339-360.
6. G. Cheng, Z. Zhang, S. F. Chen, J. D. Bryers and S. Y. Jiang, *Biomaterials*, 2007, 28, 4192-4199.
7. G. M. Manecka, J. Labrash, O. Rouxel, P. Dubot, J. Lalevée, S. A. Andaloussi, E. Renard, V. Langlois and D. L. Versace, *ACS Sustainable Chem. Eng.*, 2014, 2, 996-1006.
8. R. Poupart, A. Haider, J. Babinot, I. K. Kang, J. P. Malval, J. Lalevée, S. A. Andalloussi, V. Langlois and D. L. Versace, *ACS Biomater. Sci. Eng.*, 2015, 1, 525-538.
9. M. Ignatova, K. Starbova, N. Markova, N. Manolova and I. Rashkov, *Carbohydr. Res.* , 2006, 341, 2098-2107.
10. M. Ignatova, Z. Petkova, N. Manolova, N. Markova and I. Rashkov, *Macromol. Biosci.* , 2012, 12, 104-115.
11. S. E. Habnouni, V. Darcos, X. Garric, J.-P. Lavigne, B. Nottelet and J. Coudane, *Adv. Funct. Mater.*, 2011, 21, 3321-3330.
12. C. Lorenzini, A. Haider, I.-K. Kang, M. Sangermano, S. Abbad-Andalloussi, P.-E. Mazeran, J. Lalevée, E. Renard, V. Langlois and D.-L. Versace, *Biomacromolecules*, 2015, 16, 683-694.
13. T. T. Ruckh, R. A. Oldinski, D. A. Carroll, K. Mikhova, J. D. Bryers and K. C. Popat, *J. Mater. Sci: Mater. Med.* , 2012, 23, 1411-1420.
14. J. Lu, M. A. Hill, M. Hood, J. D. F. Greeson, J. R. Horton, P. E. Orndorff, A. S. Herndon and A. E. Tonelli, *J. Appl. Polym. Sci.*, 2001, 82, 300-309.
15. D. Chung, S. E. Papadakis and K. L. Yam, *Int. J. Food Sci. Technol.* , 2003, 38, 165-169.
16. M. L. W. Knetsch and L. H. Koole, *Polymers*, 2011, 3, 340-366.
17. Z. Markovic, B. Todorovic-Markovic, D. Kleut, N. Nikolic, S. Vranjes-Djuric, M. Misirkic, L. Vucicevic, K. Janjetovic, A. Isakovic, L. Harhaji, B. Babic-Stojic, M. Dramicanin and V. Trajkovic, *Biomaterials*, 2007, 28, 5437-5448.
18. M. J. Niedre, A. J. Secord, M. S. Patterson and B. C. Wilson, *Cancer Res.*, 2003, 63, 7986-7994.
19. X. Ragas, L. P. Cooper, J. H. White, S. Nonell and C. Flors, *ChemPhysChem*, 2011, 12, 161-165.
20. X. Ragas, M. Agut and S. Nonell, *Free Radical Biol. Med.*, 2010, 49, 770-776.
21. R. Cahan, R. Schwartz, Y. Langzam and Y. Nitzan, *Photochem. Photobiol.*, 2011, 87, 1379-1386.

22. V. Decraene, J. Pratten and M. Wilson, *Curr. Microbiol.*, 2008, 57, 269-273.
23. V. Decraene, J. Pratten and M. Wilson, *Infection Control and Hospital Epidemiology*, 2008, 29, 1181-1184.
24. S. Ismail, S. Perni, J. Pratten, I. Parkin and M. Wilson, *Infection Control and Hospital Epidemiology*, 2011, 32, 1130-1132.
25. V. Decraene, D. Ready, J. Pratten and M. Wilson, *J. Gen. Appl. Microbiol.*, 2008, 54, 195-203.
26. P. G. Calzavara-Pinton, M. Venturini and R. Sala, *J. Photochem. Photobiol. B*, 2005, 78, 1-6.
27. T. Maisch, C. Bosl, R. M. Szeimies, N. Lehn and C. Abels, *Antimicrob. Agents Chemother.*, 2005, 49, 1542-1552.
28. R. F. Donnelly, P. A. McCarron and M. M. Tunney, *Microbiol. Res.*, 2008, 163, 1-12.
29. T. A. Dahl, W. R. Midden and P. E. Hartman, *J. Bacteriol.* , 1989, 171, 2188-2194.
30. G. Jori, *J. Environ. Pathol. Toxicol. Oncol.* , 2006, 25, 505-519.
31. M. Wilson, *Infection Control and Hospital Epidemiology*, 2003, 24, 782-784.
32. A. Felgentrager, T. Maisch, A. Spath, J. A. Schroder and W. Baumler, *Phys.Chem.Chem.Phys.*, 2014, 16, 20598-20607.
33. S. Yano, S. Hirohara, M. Obata, Y. Hagiya, S.-I. Ogura, A. Ikeda, H. Kataoka, M. Tanaka and T. Joh, *J. Photochem. Photobiol. C: Photochem. Rev.*, 2011, 12, 46-67.
34. K. W. Oh, H.-M. Choi, J. M. Kim, J. H. Park and I. S. Park, *Textile Research J.*, 2014, 84, 808.
35. M. N. Usacheva, M. C. Teichert and M. A. Biel, *Lasers Surg. Med.*, 2001, 29, 165-173.
36. G. E. Cohn and H. Y. Tseng, *Photochem. Photobiol.*, 1977, 26, 465-474.
37. F. Freire, A. Costa, C. Pereira, M. Beltrame Junior, J. Junqueira and A. Jorge, *Lasers Med. Sci.*, 2014, 29, 949-955.
38. P. V. Araujo, K. I. Teixeira, L. D. Lanza, M. E. Cortes and L. T. Poletto, *Acta. Odontol. Latinoam*, 2009, 22, 93-97.
39. Y. Guo, S. Rogelj and P. Zhang, *Nanotechnology*, 2010, 21, 065102.
40. S. Dutta, S. Padhye, K. I. Priyadarsini and C. Newton, *Bioorg. Med. Chem. Lett.*, 2005, 15, 2738-2744.
41. B. B. Aggarwal, C. Sundaram, N. Malani and H. Ichikawa, *Adv. Experimental Med. Biol.*, 2007, 595, 1-75.
42. G. Bar-Sela, R. Epelbaum and M. Schaffer, *Current Med. Chem.*, 2010, 17, 190-197.
43. P. Anand, A. B. Kunnumakkara, R. A. Newman and B. B. Aggarwal, *Mol. Pharmaceutics*, 2007, 4, 807-818.
44. S. M. Khopde, K. I. Priyadarsini, D. K. Palit and T. Mukherjee, *Photochem. Photobiol.*, 2000, 72, 625-631.
45. K. I. Priyadarsini, *J. Photochem. Photobiol. C*, 2009, 10, 81-95.
46. H.-J. Kim, D.-J. Kim, S. N. Karthick, K. V. Hemalatha, C. J. Raj, S. Ok and Y. Choe, *Int. J. Electrochem. Sci.*, 2013, 8, 8320-8329.
47. J. Zhao, J. Lalevée, H. Lu, R. MacQueen, S. H. Kable, T. W. Schmidt, M. H. Stenzel and P. Xiao, *Polym. Chem.*, 2015, 6, 5053-5061.
48. J. V. Crivello and U. Bulut, *J. Polym. Sci. Part A: Polym. Chem.*, 2005, 43, 5217-5231.
49. J. V. Crivello and U. Bulut, *Macromol. Symp.*, 2006, 240, 1-11.
50. M. Jin, J. Xie, J.-P. Malval, A. Spangenberg, O. Soppera, D.-L. Versace, T. Leclerc, H. Pan, D. Wan, H. Pu, P. Baldeck, O. Poizat and S. Knopf, *J. Mater. Chem. C*, 2014, 2, 7201-7215.
51. G. Pohlers, J. C. Scaiano and R. Sinta, *Chem. Mater.*, 1997, 9, 3222-3230.
52. D. Rehm and A. Weller, *Isr. J. Chem.*, 1970, 8, 259-271.
53. J.-P. Fouassier and J. Lalevée, *Photoinitiators for Polymer Synthesis: Scope, Reactivity and Efficiency*, Wiley-VCH Verlag GmbH and Co KGaA, Weinheim, 2012.
54. T. A. Dahl, W. R. Midden and P. E. Hartman, *Photochem. Photobiol.*, 1987, 46, 345-352.
55. D. Bellus, H. Lind and J. F. Wyatt, *J. Chem. Soc., Chem. Commun.*, 1972, 1199-1200.
56. G. Gryn'ova, K. U. Ingold and M. L. Coote, *J. Am. Chem. Soc.*, 2012, 134, 12979-12988.
57. A. Gomes, E. Fernandes and J. L. F. C. Lima, *J. Biochem. Biophys. Methods*, 2005, 65, 45-80.
58. M. C. DeRosa and R. J. Crutchley, *Coord. Chem. Rev.*, 2002, 233–234, 351-357.
59. D. J. Balazs, K. Triandafillu, P. Wood, Y. Chevolot, C. v. Delden, H. Harms, C. Hollensteind and H. J. Mathieu, *Biomaterials*, 2004, 25, 2139–2151.
60. P. J. Eginton, H. Gibson, J. Holah, P. S. Handley and P. Gilbert, *J. Ind. Microbiol.*, 1995, 15, 305-310.
61. W. Zhou, S. M. Kuebler, D. Carrig, J. W. Perry and S. R. Marder, *J. Am. Chem. Soc.*, 2002, 124, 1897-1901.
62. M. Montalti, A. Credi, L. Prodi and M. T. Gandolfi, CRC Press, Boca Raton, 3rd edn., 2006.

Journal Name

ARTICLE

TABLE of CONTENT

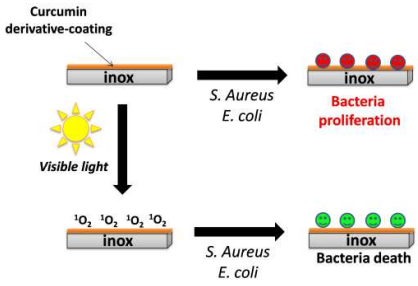

Synthesis of antibacterial coatings derived from epoxidized soybean oil and curcumin for the efficient inhibition of bacteria proliferation.